VOLUME 120, NUMBER 18
MAY 13, 1998

JOURNAL OF THE AMERICAN CHEMICAL SOCIETY

Insights into the Solvent Dependence of Chymotryptic Prochiral Selectivity

Tao Ke and Alexander M. Klibanov*

Contribution from the Department of Chemistry, Massachusetts Institute of Technology, Cambridge, Massachusetts 02139

Received January 20, 1998

Abstract: In a previous publication (Ke, T.; Wescott, C. R.; Klibanov, A. M. *J. Am. Chem. Soc.* **1996**, *118*, 3366−3374), we discovered and rationalized mechanistically a marked solvent dependence of chymotrypsin's prochiral selectivity in the acylation of 2-(3,5-dimethoxybenzyl)-1,3-propanediol with vinyl acetate. In this study, we have answered several important unresolved questions concerning that phenomenon. It has been found that the solvent dependence of prochiral selectivity is dominated by that of $(k_{cat}/K_M)_{pro-R}$, and this finding has been explained on the basis of a computer modeling analysis of *pro-R* and *pro-S* transition-state structures. There is no correlation between the solvent-induced changes of k_{cat}/K_M values and those of either k_{cat} or K_M individually, presumably reflecting the complex nature of the latter two parameters. Finally, the observed metamorphosis of chymotrypsin from a nonselective to a highly selective catalyst upon variation in the solvent is *not* attained at the expense of lowered enzymatic reactivity; in fact, prochiral selectivity and catalytic efficiency seem to rise concomitantly.

Introduction

Our discovery[1] that enzymatic stereoselectivity is a strong function of the reaction medium is the highlight of nonaqueous enzymology[2] which promises greater synthetic applications of enzymes.[3] In particular, prochiral selectivity of enzymes is markedly affected by the solvent.[4,5] For example, prochiral selectivity of crystalline chymotrypsin in the acylation of 2-(3,5-dimethoxybenzyl)-1,3-propanediol (**1**) with vinyl acetate can be inversed and forced to change more than an order of magnitude merely by varying the solvent under otherwise identical conditions.[5] We have been able to mechanistically and almost quantitatively account for this effect on the basis of the differential energetics of substrate desolvation in the *pro-R* and *pro-S* enzyme-bound transition states.[5]

That study,[5] however, left several important issues unresolved. Because of the experimental methodology employed, only the $(k_{cat}/K_M)_{pro-R}/(k_{cat}/K_M)_{pro-S}$ ratios (i.e., prochiral selectivities[6]), as opposed to the individual k_{cat}/K_M values for each stereochemical route, were determined as a function of the solvent. Consequently, it is unknown whether the aforementioned solvent dependence of chymotrypsin's prochiral selectivity is mainly due to that of $(k_{cat}/K_M)_{pro-R}$ or $(k_{cat}/K_M)_{pro-S}$. Likewise, are the

(1) Wescott, C. R.; Klibanov, A. M. *Biochim. Biophys. Acta* **1994**, *1206*, 1−9. Carrea, G.; Ottolina, G.; Riva, S. *Trends Biotechnol.* **1995**, *13*, 63−70.

(2) Koskinen, A. M. P.; Klibanov, A. M., Eds.; *Enzymatic Reactions in Organic Media*; Blackie: London, 1996.

(3) Poppe, L.; Novak, L. *Selective Biocatalysis*; VCH Publishers: New York, 1992. Wong, C.-H.; Whitesides, G. M. *Enzymes in Synthetic Organic Chemistry*; Pergamon: Oxford, 1994. Drauz, K.; Waldmann, H. *Enzyme Catalysis in Organic Synthesis*; VCH Publishers: New York, 1995. Faber, K. *Biotransformations in Organic Chemisry*; Springer-Verlag: Berlin, 1996.

(4) Hirose, Y.; Kariya, K.; Sasaki, I.; Kurono, Y.; Ebiike, H.; Achiwa, K. *Tetrahedron Lett.* **1992**, *33*, 7157−7160. Terradas, F.; Teston-Henry, M.; Fitzpatrick, P. A.; Klibanov, A. M. *J. Am. Chem. Soc.* **1993**, *115*, 390−396. Faber, K.; Ottolina, G.; Riva, S. *Biocatalysis* **1993**, *8*, 91−132.

(5) Ke, T.; Wescott, C. R.; Klibanov, A. M. *J. Am. Chem. Soc.* **1996**, *118*, 3366−3374.

(6) Chen, C.-S.; Fujimoto, Y.; Girdaukas, G.; Sih, C. J. *J. Am. Chem. Soc.* **1982**, *104*, 7294−7299. Straathof, A. J. J.; Jongejan, J. A. *Enzyme Microbial Technol.* **1997**, *21*, 559−571.

S0002-7863(98)00220-0 CCC: $15.00
Published on Web 04/28/1998

Scheme 1

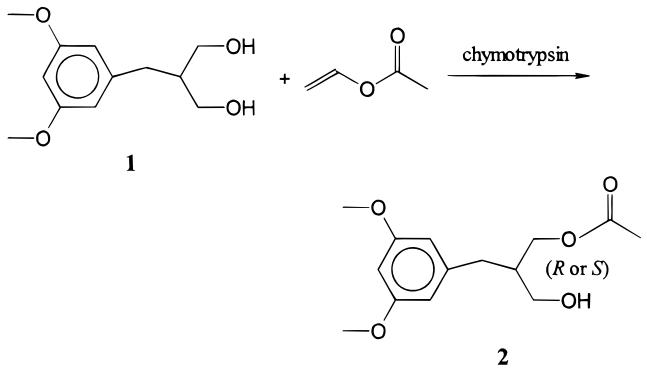

1 **2**

solvent-dependent changes in k_{cat} or in K_M the chief contributors to the observed solvent effects? Finally, while intuitively it seems plausible that a solvent-induced enhancement of enzymatic prochiral selectivity would be attained at the expense of lower absolute reactivity, is this really the case? The present study provides answers to all of these questions.

Results and Discussion

The enzymatic transesterification reaction examined herein is depicted in Scheme 1. Crystalline chymotrypsin was selected as a catalyst because its X-ray structure is almost the same in aqueous and nonaqueous solvents[7] thus allaying concerns about solvent-induced conformational changes and allowing structure-based computer modeling. The progress of the reaction was monitored by chiral HPLC which afforded a facile discrimination between the (*R*) and (*S*) monoacetyl products **2**. The initial rates of their formation in various organic solvents were measured as a function of the initial concentration of the prochiral nucleophile **1**, and the data obtained were plotted in double-reciprocal coordinates to determine k_{cat} and K_M values for both *pro-R* and *pro-S* reaction pathways. Table 1 lists these parameters, as well as the k_{cat}/K_M values derived from them and the resultant $(k_{cat}/K_M)_{pro-R}/(k_{cat}/K_M)_{pro-S}$ ratios, in 11 organic solvents. Note that the prochiral selectivity values in Table 1 are overall similar to those[5] obtained in a different way in our earlier study.

We demonstrated previously[5] that the solvent dependence of prochiral (as well as of some other types, e.g., enantiomeric[8]) selectivity can be described by the following equation:

$$\log[(k_{cat}/K_M)_{pro-R}/(k_{cat}/K_M)_{pro-S}] = \log(\gamma'_{pro-R}/\gamma'_{pro-S}) + \text{constant} \quad (1)$$

where γ' is the thermodynamic activity coefficient of the desolvated portion of the substrate in the corresponding enzyme-bound transition state. Figure 1 depicts the dependence of chymotrypsin's prochiral selectivity values from Table 1 on the γ' ratio (calculated by means of molecular modeling and the UNIFAC computer algorithm; see the Experimental Section); the expected linear correlation with a slope of unity is indeed observed. Therefore, having determined the individual kinetic parameters (Table 1), we were now in the position to address the questions outlined in the Introduction.

Even a cursory inspection of the Table 1 data reveals that $(k_{cat}/K_M)_{pro-R}$ makes a much greater contribution to the solvent dependence of prochiral selectivity than $(k_{cat}/K_M)_{pro-S}$. For example, upon transition from diisopropyl ether to the solvent on the other extreme in the table, acetonitrile, when prochiral selectivity slumps 32-fold, the enzymatic reactivity in the *pro-R* route also drops 20-fold, whereas that in the *pro-S* rises just

Table 1. Individual Kinetic Parameters for the Acylation of **1** Catalyzed by Crystalline Chymotrypsin in Various Organic Solvents[a]

solvent	stereochem. route	$10^2 k_{cat}$ (h^{-1})	K_M (mM)	$10^3(k_{cat}/K_M)$ ($mM^{-1}\,h^{-1}$)	$(k_{cat}/K_M)_{pro-R}/(k_{cat}/K_M)_{pro-S}$
diisopropyl ether	*pro-R*	8.1 ± 0.7	4.5 ± 1.2	18 ± 3	16 ± 4
	pro-S	1.3 ± 0.2	12 ± 4	1.1 ± 0.1	
dibutyl ether	*pro-R*	7.4 ± 0.7	7.7 ± 1.6	9.6 ± 1.2	8.0 ± 1.7
	pro-S	1.2 ± 0.2	9.9 ± 2.9	1.2 ± 0.2	
tert-butyl acetate	*pro-R*	3.2 ± 0.2	11 ± 2	2.9 ± 0.2	3.1 ± 0.7
	pro-S	0.97 ± 0.14	11 ± 4	0.92 ± 0.17	
dioxane	*pro-R*	4.1 ± 0.5	12 ± 3	3.4 ± 0.5	2.7 ± 0.7
	pro-S	1.6 ± 0.2	13 ± 3	1.3 ± 0.2	
cyclohexane	*pro-R*	n.d.[b]	n.d.[b]	5.0 ± 0.7	2.6 ± 0.8
	pro-S	n.d.[b]	n.d.[b]	1.9 ± 0.3	
tetrahydrofuran	*pro-R*	2.2 ± 0.3	12 ± 4	1.9 ± 0.3	2.1 ± 0.8
	pro-S	1.0 ± 0.2	11 ± 4	0.91 ± 0.19	
p-xylene	*pro-R*	1.4 ± 0.4	6.5 ± 2.3	2.1 ± 0.2	1.2 ± 0.3
	pro-S	1.4 ± 0.5	7.8 ± 3.5	1.8 ± 0.2	
toluene	*pro-R*	0.87 ± 0.07	3.7 ± 0.5	2.4 ± 0.2	1.1 ± 0.1
	pro-S	0.89 ± 0.10	4.1 ± 0.7	2.2 ± 0.1	
methyl acetate	*pro-R*	15 ± 6	51 ± 24	2.9 ± 0.5	0.93 ± 0.25
	pro-S	27 ± 14	87 ± 52	3.1 ± 0.5	
propionitrile	*pro-R*	2.7 ± 0.7	24 ± 9	1.1 ± 0.2	0.55 ± 0.17
	pro-S	3.9 ± 1.0	20 ± 7	2.0 ± 0.3	
acetonitrile	*pro-R*	3.2 ± 0.7	35 ± 8	0.91 ± 0.07	0.50 ± 0.08
	pro-S	6.0 ± 1.2	33 ± 9	1.8 ± 0.2	

[a] The conditions and the way the determinations were carried out are described in the Experimental Section. The errors shown were directly derived from the linear fitting using SigmaPlot. The k_{cat} and K_M listed correspond to the catalytic and Michaelis constant, respectively, for **1**. [b] Not determined. The K_M values in cyclohexane were much greater than the solubility of **1**; therefore, the individual kinetic constants could not be determined.

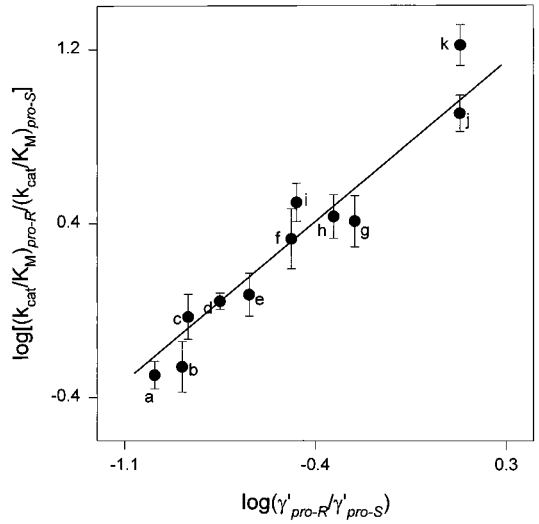

Figure 1. Dependence of the prochiral selectivity of crystalline chymotrypsin in the acylation of **1** (Scheme 1) in various organic solvents on the ratio of the thermodynamic activity coefficients of the desolvated portions of the substrate in the *pro-R* and *pro-S* transition states (eq 1).[11] Solvents: (a) acetonitrile, (b) propionitrile, (c) methyl acetate, (d) toluene, (e) *p*-xylene, (f) tetrahydrofuran, (g) cyclohexane, (h) dioxane, (i) *tert*-butyl acetate, (j) dibutyl ether, and (k) diisopropyl ether. The straight line drawn, with the forced theoretically predicted slope of unity (eq 1), has a correlation coefficient of 0.89. For conditions and methods, see the Experimental Section.

(7) Yennawar, N. H.; Yennawar, H. P.; Farber, G. K. *Biochemistry* **1994**, *33*, 7326−7336. Yennawar, H. P.; Yennawar, N. H.; Farber, G. K. *J. Am. Chem. Soc.* **1995**, *117*, 577−585.

(8) Wescott, C. R.; Noritomi, H.; Klibanov, A. M. *J. Am. Chem. Soc.* **1996**, *118*, 10365−10370.

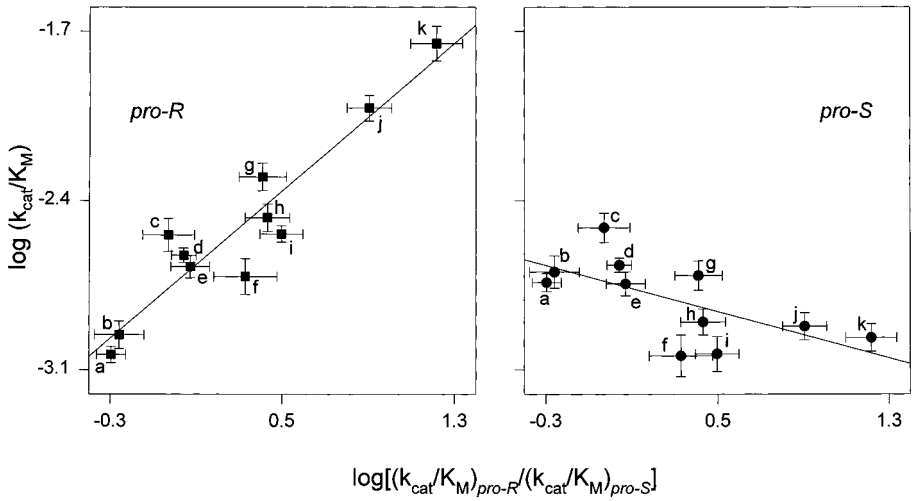

Figure 2. The $(k_{cat}/K_M)_{pro-R}$ (left) and $(k_{cat}/K_M)_{pro-S}$ (right) values plotted against the prochiral selectivity of crystalline chymotrypsin in the acylation of **1** (Scheme 1) in various organic solvents.[11] Solvents: see the legend to Figure 1. The straight lines, drawn using linear regression, have slopes of 0.75 and −0.25 for the *pro-R* and *pro-S* stereochemical route, respectively. For conditions and methods, see the Experimental Section.

1.6-fold. Moreover, this conclusion is supported by the entire body of the experimental data in Figure 2, where k_{cat}/K_M values for the *pro-R* and *pro-S* route are separately plotted against the prochiral selectivities in the corresponding solvents. One can see that the absolute value of the slope for the former exceeds that for the latter by a factor of 3 in double-logarithmic coordinates.

These findings can be rationalized on the basis of the molecular modeling results depicted in Figures 3 and 4. Figures 3A and 4A show **1** covalently bound to the active site of chymotrypsin in the *pro-R* and *pro-S* transition states, respectively. From these, one can identify the desolvated portions of the substrate in both transition states (nondotted moieties in Figures 3B and 4B). It is seen that, to the first approximation, what is desolvated in the *pro-S* transition state, is also desolvated in the *pro-R*. However, the 3,5-dimethoxyphenyl moiety, while solvated in the *pro-S* transition state, is desolvated in the *pro-R*. Since the contributions of the identical groups to the γ'_{pro-R} and γ'_{pro-S} in eq 1 approximately cancel out,[9] the solvent dependence of prochiral selectivity should be dominated by that of the *pro-R* pathway, which is indeed the case (Figure 2).

The next question was whether the solvent dependence of $(k_{cat}/K_M)_{pro-R}$ primarily stems from that of k_{cat} or K_M or neither. To answer, we plotted the $(k_{cat}/K_M)_{pro-R}$ values in various solvents against k_{cat} (Figure 5A) and K_M (Figure 5B) values in the same solvents. One can see that no discernible correlation exists for either parameter. This is presumably because both k_{cat} and K_M for enzymatic transesterifications in organic solvents, such as that in Scheme 1, are complex, multicomponent parameters.[10] It is worth noting that a similar lack of correlation was also observed for the solvent dependence of the *pro-S* route (Figure 5C and 5D).

In the bottom six solvents in Table 1, chymotrypsin's prochiral selectivity is low: neither stereochemical route is favored by more than 2-fold. In contrast, in the top two solvents, the *pro-R* pathway is preferred over the *pro-S* by some order of magnitude. In other words, such a change in the reaction medium converts the enzyme from an essentially nonselective to a very selective catalyst. A question arises whether this metamorphosis occurs at the expense of a reduced chymotryptic activity. To answer it, we plotted the prochiral selectivity in different solvents versus the sum of k_{cat}/K_M values for *pro-R* and *pro-S* pathways in the same solvents (this sum was used as

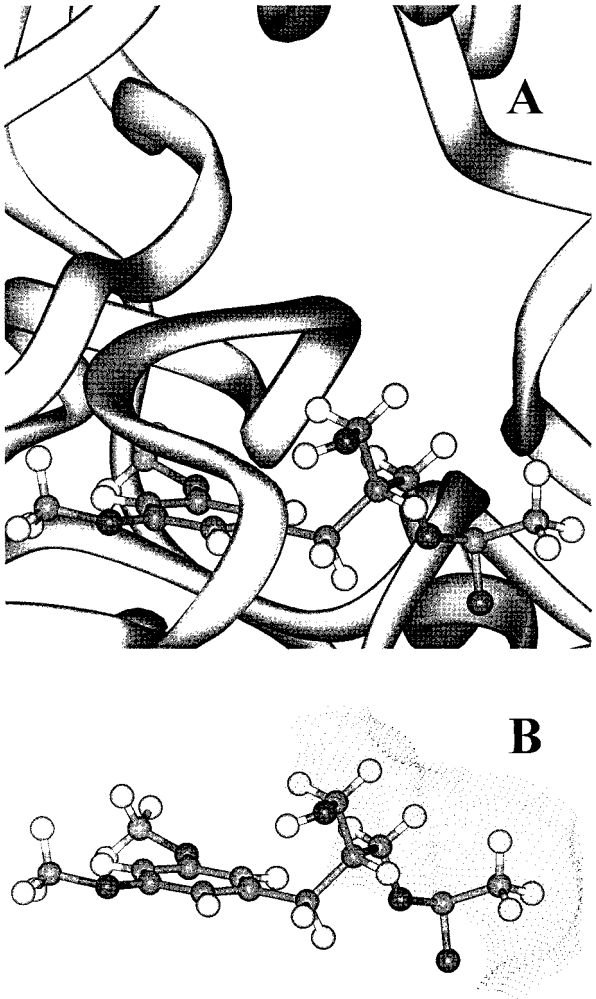

Figure 3. Conformation (A) and solvent-accessible surface area (B) of substrate **1** in the *pro-R* transition state with chymotrypsin. (A) The main chain of chymotrypsin in the active site region is depicted as a ribbon diagram, and the substrate is represented by a ball-and-stick model. (B) The dots demarcate the solvent-accessible surfaces calculated using the Connolly method. See the Experimental Section for details.

(9) Wescott, C. R.; Klibanov, A. M. *J. Am. Chem. Soc.* **1993**, *115*, 10362−10363.

(10) Chatterjee, S.; Russell, A. J. *Biotechnol. Bioeng.* **1992**, *40*, 1069−1077.

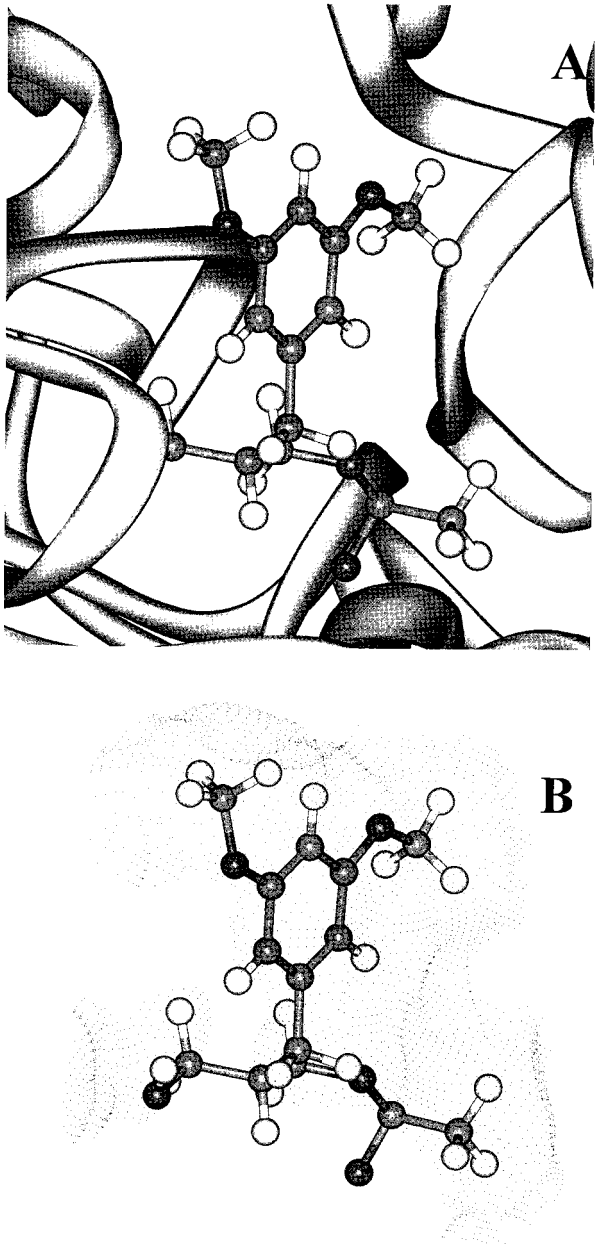

Figure 4. Conformation (A) and solvent-accessible surface area (B) of substrate **1** in the *pro-S* transition state with chymotrypsin. (A) The main chain of chymotrypsin in the active site region is depicted as a ribbon diagram, and the substrate is represented by a ball-and-stick model. (B) The dots demarcate the solvent-accessible surfaces calculated using the Connolly method. See the Experimental Section for details.

a measure of the overall enzymatic potency). The resultant graph[11] (Figure 6) reveals not a hint of a systematic decline in enzymatic reactivity as prochiral selectivity undergoes a solvent-induced rise. In fact, the trend seems to be just the opposite, i.e., the activity and selectivity ascend together. This phenomenon, if general, bodes well for the prospect of making enzymes both more selective and more active by optimizing the solvent.

Experimental Section

Materials. Bovine pancreatic α-chymotrypsin (EC 3.4.21.1), crystallized three times (Type II), was purchased from Sigma Chemical Company. γ-Chymotrypsin crystals were obtained from the α-form of the enzyme following the method of Stoddard et al.[12] For use in organic solvents, the crystals were lightly cross-linked with glutaraldehyde and prepared for catalysis as described previously.[5] Chemicals were from Aldrich Chemical Company and were of analytical grade or purer. All organic solvents were purchased from commercial suppliers in the anhydrous state and were of the highest purity available. The prochiral diol **1** and its monoacetylated ester **2** were synthesized using the procedure described previously[5] and verified by ^{1}H NMR.

Kinetic Measurements. One milliliter of a solvent containing 100 mM vinyl acetate and various concentrations of **1** was added to 5 mg of cross-linked enzyme crystals, and then 0.2% (v/v) water was added to the suspension to enhance the rate of enzymatic transesterfication.[5]

(11) Throughout this paper, we use double-logarithmic coordinates to give equal weight to all experimental points. Given a wide range in which the measured parameters vary (Table 1), linear coordinates would not afford such a possibility.

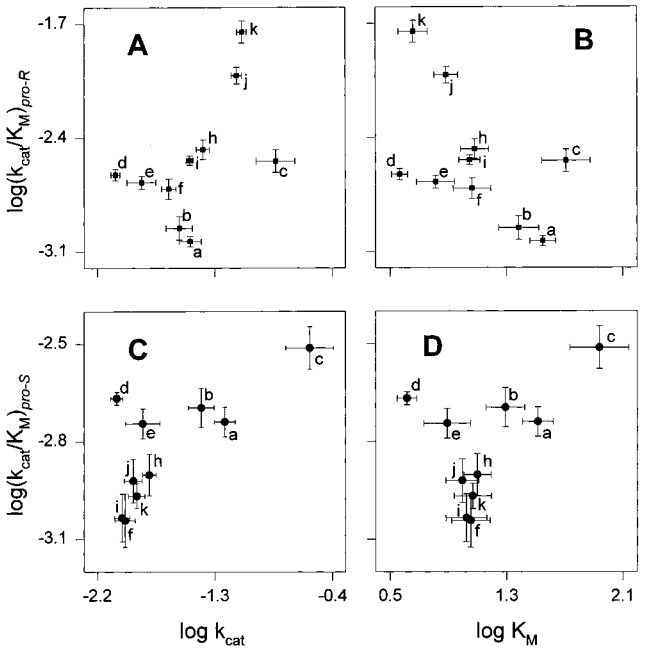

Figure 5. The $(k_{cat}/K_M)_{pro-R}$ and $(k_{cat}/K_M)_{pro-S}$ as a function of the individual k_{cat} and K_M values for the acylation of **1** (Scheme 1) catalyzed by crystalline chymotrypsin in various organic solvents.[11] Solvents: see the legend to Figure 1, except that cyclohexane (g), where the individual k_{cat} and K_M values could not be determined, is missing. For conditions and methods, see the Experimental Section.

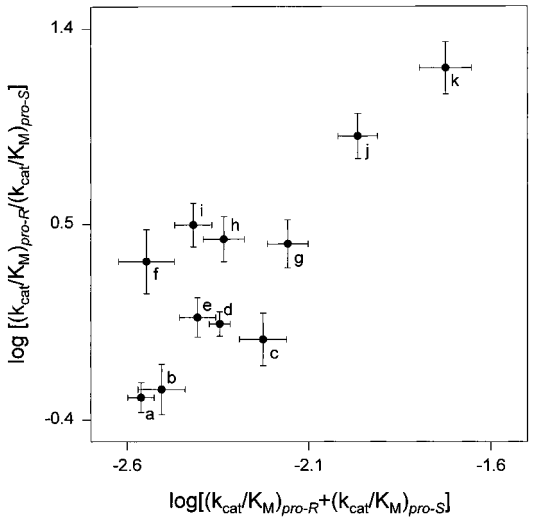

Figure 6. The prochiral selectivity of crystalline chymotrypsin in the acylation of **1** (Scheme 1) in various organic solvents plotted against the sum of the k_{cat}/K_M values for *pro-R* and *pro-S* stereochemical routes. For conditions and methods, see the Experimental Section.

(12) Stoddard, B. L.; Bruhnke, J.; Porter, N.; Ringe, D.; Petsko, G. A. *Biochemistry* **1990**, *29*, 4871−4876.

(In the presence of the dissolved substrates, this amount of added water was soluble in each of the solvents used.) The suspensions were shaken at 30 °C and 300 rpm. Periodically, a 5-μL sample was withdrawn and assayed by chiral HPLC using a Chiralcel OD-H column (Chiral Technologies, Inc.) and a mobile phase consisting of 95:5 (v/v) hexane: 2-propanol at a flow rate of 0.8 mL/min. The chemically synthesized racemic mixture of **2,** eluted with retention times of 29 and 32 min for the (*R*) and (*S*) enantiomers, respectively, was used to precalibrate the HPLC UV detector tuned to 220 nm.

Kinetic parameters (Table 1) of the chymotrypsin-catalyzed transesterification (Scheme 1) were measured by varying the concentration of the nucleophile, **1**, in the range of 1.6−100 mM, depending on the K_M value. Initial rate data were fitted to the Michaelis−Menten equation using the Lineweaver−Burk double reciprocal fit (SigmaPlot, Jandel Scientific). The linear correlation coefficients, R^2, obtained in various solvents were as follows (for the *pro-R* and *pro-S* stereochemical route, respectively): diisopropyl ether 0.92, 0.89; dibutyl ether 0.92, 0.95; *tert*-butyl acetate 0.85, 0.97; dioxane 0.93, 0.92; cyclohexane 0.91, 0.89; tetrahydrofuran 0.81, 0.85; *p*-xylene 0.93, 0.94; toluene 0.97, 0.98; methyl acetate 0.93, 0.91; propionitrile 0.88, 0.91; acetonitrile 0.96, 0.97.

Active Site Titration. The percentage of the catalytically competent chymotrypsin molecules in organic solvents (used to calculate $[E]_0$ in the Michaelis−Menten equation) was determined by titrating the active sites in the corresponding solvents with an irreversible serine protease inhibitor, phenylmethylsufonyl fluoride (PMSF), as described previously.[13] Cross-linked enzyme crystals (25 mg/mL) were placed in 2 mL of the solvent containing 1 mM PMSF, and the suspension was shaken at 30 °C and 300 rpm. The disappearance of PMSF, as well as any spontaneous hydrolysis product, was monitored by HPLC. Titration of thermoinactivated γ-chymotrypsin under identical conditions was used as the blank reference. Titration in three representative solvents of those listed in Table 1, diisopropyl ether, dioxane, and acetonitrile, done in quadruplicate to avoid random errors, yielded values statistically indistiguishable from each other: 22 ± 6%, 16 ± 4%, and 21 ± 7%, respectively. Given this fact, and that the titration requires a large amount of cross-linked enzyme crystals, the average value of these titration data, 20 ± 5%, was used in all k_{cat} and k_{cat}/K_M calculations presented in Table 1.

(13) Schmitke, J. L.; Wescott, C. R.; Klibanov, A. M. *J. Am. Chem. Soc.* **1996**, *118*, 3360−3365.

Structural Modeling. Molecular models of the *pro-R* and *pro-S* transition states for the enzymatic transesterification in Scheme 1 were produced using the crystal structure of γ-chymotrypsin in hexane (Brookhaven data bank entry 1GMC).[7] The tetrahedral intermediates in the deacylation step of the enzymatic reaction were selected as the models of the transition state.[14] Such models were produced using the two-step procedure outlined below and described in detail previously.[5] First, potential binding modes of each enantiomeric product ((*R*) or (*S*) **2**) to the enzyme were generated by performing molecular dynamics simulations, followed by energy minimization. The carbonyl oxygen of the product was tethered to the oxyanion binding site using a harmonic potential with a force constant selected to allow widely different conformations to be explored, while preventing the product from diffusing too far from the enzyme. Second, each product binding mode thus identified was used as a template for creating an initial model of the tetrahedral intermediate. The lowest-energy conformer found thereafter using molecular dynamics simulations and energy minimization was selected as the model of the transition state (Figures 3A and 4A), from which the solvent-accessible surface (Figures 3B and 4B) was calculated by the method of Connolly.[15]

Activity Coefficient Calculation. All thermodynamic activity coefficients (γ' in eq 1) were calculated using the UNIFAC method.[5,16] All such calculations explicitly included the effects of 100 mM vinyl acetate and 0.2% (v/v) water.

Acknowledgment. This work was financially supported by a grant from the National Science Foundation. We are grateful to Dr. Charles R. Wescott for helpful discussions and to Profs. Gregory A. Petsko and Gregory K. Farber for providing chymotrypsin seed crystals.

JA9802201

(14) Warshel, A.; Naray-Szabo, G.; Sussman, F.; Hwang, J.-K. *Biochemistry* **1989**, *28*, 3629−3637.

(15) Connolly, M. L. *Science* **1983**, *221*, 709−712.

(16) Fredenslund, A.; Gmehling, J.; Rasmussen, P. *Vapor-Liquid Equilibria Using UNIFAC*; Elsevier: New York, 1977. Steen, S.-J.; Bärbel, K.; Gmehling, J.; Rasmussen, P. *Ind. Eng. Chem. Proc. Des. Dev.* **1979**, *18*, 714−722. Gmehling, J.; Rasmussen, P.; Fredenslund, A. *Ind. Eng. Chem. Proc. Des. Dev.* **1982**, *21*, 118−127. Macedo, E. A.; Weidlich, U.; Gmehling, J.; Rasmussen, P. *Ind. Eng. Chem. Proc. Des. Dev.* **1983**, *22*, 676−678. Tiegs, D.; Gmehling, J.; Rasmussen, P.; Fredenslund, A. *Ind. Eng. Chem. Proc. Des. Dev.* **1987**, *26*, 159−161. Hansen, H. K.; Rasmussen, P.; Schiller, M.; Gmehling, J. *Ind. Eng. Chem. Res.* **1991**, *30*, 2352−2355.